Solute carrier family 9, subfamily A, member 3 *(SLC9A3)*/sodium-hydrogen exchanger member 3 (NHE3) dysregulation and dilated intercellular spaces in patients with eosinophilic esophagitis

Chang Zeng, BSc,[a] Simone Vanoni, PhD,[a,e] David Wu, PhD,[a] Julie M. Caldwell, PhD,[a] Justin C. Wheeler, MD,[c] Kavisha Arora, PhD,[b] Taeko K. Noah, PhD,[a] Lisa Waggoner, BSc,[a] John A. Besse, BSc,[a] Amnah N. Yamani, BSc,[a] Jazib Uddin, BSc,[a] Mark Rochman, PhD,[a] Ting Wen, PhD,[a] Mirna Chehade, MD,[f] Margaret H. Collins, MD,[c] Vincent A. Mukkada, MD,[d] Philip E. Putnam, MD,[d] Anjaparavanda P. Naren, PhD,[b] Marc E. Rothenberg, MD, PhD,[a] and Simon P. Hogan, PhD[a,g] *Cincinnati, Ohio, Salzburg, Austria, New York, NY, and Ann Arbor, Mich*

GRAPHICAL ABSTRACT

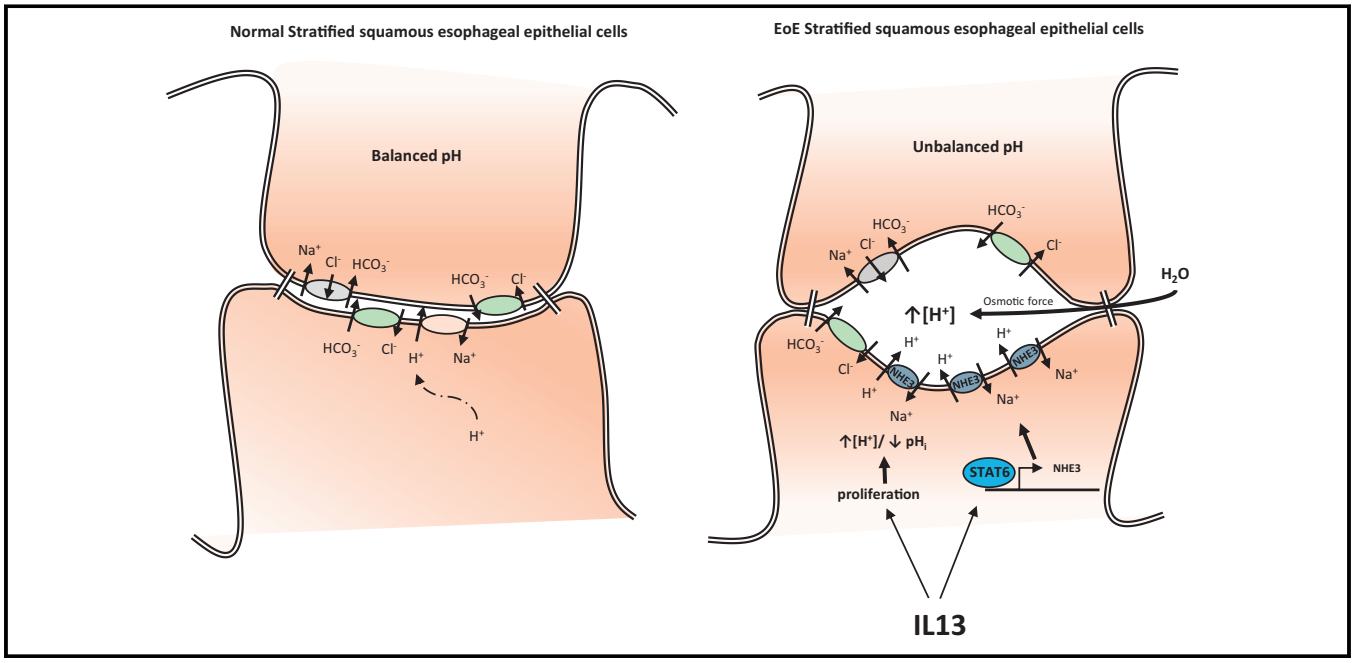

Background: Eosinophilic esophagitis (EoE) is characterized by histopathologic modifications of esophageal tissue, including eosinophil-rich inflammation, basal zone hyperplasia, and dilated intercellular spaces (DIS). The underlying molecular processes that drive the histopathologic features of EoE remain largely unexplored.

Objective: We sought to investigate the involvement of solute carrier family 9, subfamily A, member 3 (SLC9A3) in

From the Divisions of [a]Allergy and Immunology, [b]Pulmonary Medicine, [c]Pathology and Laboratory Medicine, and [d]Gastroenterology, Nutrition and Hepatology, Cincinnati Children's Hospital Medical Center; [e]the Institute of Pharmacology and Toxicology, Paracelsus Medical University, Salzburg; [f]Mount Sinai Center for Eosinophilic Disorders, Jaffe Food Allergy Institute, Icahn School of Medicine at Mount Sinai, New York; and [g]the Department of Pathology, Mary H Weiser Food Allergy Center, Michigan Medicine, University of Michigan, Ann Arbor.

Supported by National Institutes of Health grants DK090119 and AI112626, Food Allergy Research & Education, and the Crohn's Colitis Foundation of America (to S.P.H.).

Disclosure of potential conflict of interest: M. H. Collins is a consultant for Shire and Actelion and has received research grant support from Shire, Regeneron, and Nutricia. M. E. Rothenberg is a consultant for Immune Pharmaceuticals, NKT Therapeutics, PulmOne, Celgene, Shire, GlaxoSmithKline, AstraZeneca, and Novartis and has an equity interest in the first 3 companies listed and royalties from reslizumab (Teva Pharmaceuticals); he is an inventor of several patents owned by Cincinnati Children's, and a set of these patents relates to molecular diagnostics. The rest of the authors declare that they have no relevant conflicts of interest.

Received for publication August 28, 2017; revised March 15, 2018; accepted for publication March 26, 2018.

Available online May 4, 2018.

Corresponding author: Simon P. Hogan, PhD, Department of Pathology, Mary H Weiser Food Allergy Center, Michigan Medicine, University of Michigan, 109 Zina Pitcher Place, Ann Arbor, MI 48109-2200. E-mail: sihogan@med.umich.edu.

The CrossMark symbol notifies online readers when updates have been made to the article such as errata or minor corrections

0091-6749/$36.00

https://doi.org/10.1016/j.jaci.2018.03.017

esophageal epithelial intracellular pH (pH_i) and DIS formation and the histopathologic features of EoE.
Methods: We examined expression of esophageal epithelial gene networks associated with regulation of pH_i in the EoE transcriptome of primary esophageal epithelial cells and an *in vitro* esophageal epithelial 3-dimensional model system (EPC2-ALI). Molecular and cellular analyses and ion transport assays were used to evaluate the expression and function of SLC9A3.
Results: We identified altered expression of gene networks associated with regulation of pH_i and acid-protective mechanisms in esophageal biopsy specimens from pediatric patients with EoE (healthy subjects, n = 6; patients with EoE, n = 10). The most dysregulated gene central to regulating pH_i was *SLC9A3*. *SLC9A3* expression was increased within the basal layer of esophageal biopsy specimens from patients with EoE, and expression positively correlated with disease severity (eosinophils/high-power field) and DIS (healthy subjects, n = 10; patients with EoE, n = 10). Analyses of esophageal epithelial cells revealed IL-13–induced, signal transducer and activator of transcription 6–dependent *SLC9A3* expression and Na^+-dependent proton secretion and that SLC9A3 activity correlated positively with DIS formation. Finally, we showed that IL-13–mediated, Na^+-dependent proton secretion was the primary intracellular acid-protective mechanism within the esophageal epithelium and that blockade of SLC9A3 transport abrogated IL-13–induced DIS formation.
Conclusions: SLC9A3 plays a functional role in DIS formation, and pharmacologic interventions targeting SLC9A3 function may suppress the histopathologic manifestations in patients with EoE. (J Allergy Clin Immunol 2018;142:1843-55.)

Key words: *Solute carrier family 9, subfamily A, member 3/sodium-hydrogen exchanger member 3, ion transport, eosinophilic esophagitis, dilated intercellular spaces, IL-13*

Abbreviations used
ALI: Air-liquid interface
BZH: Basal zone hyperplasia
CAPN14: Calpain 14
CCHMC: Cincinnati Children's Hospital Medical Center
DIS: Dilated intercellular spaces
DMSO: Dimethyl sulfoxide
EoE: Eosinophilic esophagitis
GERD: Gastroesophageal reflux disease
GO: Gene Ontology
H&E: Hematoxylin and eosin
hpf: High-power field
IF: Immunofluorescence
KSFM: Keratinocyte serum-free media
LRRC31: Leucine-rich repeat–containing protein 31
NHE1: Sodium-hydrogen exchanger member 1
NHE3: Sodium-hydrogen exchanger member 3
pH_i: Intracellular pH
qRT-PCR: Quantitative RT-PCR
RNAseq: RNA sequencing
shRNA: Short hairpin RNA
SLC9A3: Solute carrier family 9, subfamily A, member 3
STAT: Signal transducer and activator of transcription

Eosinophilic esophagitis (EoE) is a food allergen–induced inflammatory disease that is increasing in incidence (5-10 cases per 100,000) and prevalence (0.5-1 case per 1000).[1-4] Common symptoms of EoE include vomiting, dysphagia, chest pain, food impaction, and upper abdominal pain[5] and decreased health-related quality of life.[6]

Corroborative clinical and experimental studies indicate that an underlying allergic sensitization to dietary food antigens and development of a $CD4^+$ T_H2 and type 2 innate lymphoid cell inflammatory response in the esophageal mucosa drive eosinophilic inflammation and esophageal remodeling in patients with EoE, which includes basal zone hyperplasia (BZH) and dilated intercellular spaces (DIS).[7-10] Dietary modification (ie, complete or targeted food antigen avoidance) and swallowed glucocorticoids alleviate much of the disease pathology,[11,12] suggesting a food-induced $CD4^+$ type 2 allergic inflammatory response.[13-18]

Consistent with this, animal-based studies have revealed important roles for $CD4^+$ T_H2 cells, proallergic cytokines (IL-5 and IL-13), and eosinophils in the histopathologic manifestations of disease.[19-21] One cytokine that seems to be central in orchestrating the EoE phenotype is IL-13.[22-24] IL-13 is highly upregulated in esophageal tissue of patients with EoE and is sufficient to alter gene expression in esophageal epithelial cells *in vitro* and *in vivo*, and the IL-13–induced transcriptome significantly overlaps with transcriptional changes observed in esophageal biopsy specimens of patients with EoE.[22-24] Importantly, treating patients with EoE with a humanized antibody against IL-13 led to a significant decrease in esophageal eosinophil counts and had a normalizing effect on the dysregulated transcriptome observed in patients with EoE.[25] IL-13 has been shown to dysregulate the expression of several key epithelial barrier regulatory genes, including desmosomal cadherin, desmoglein-1, leucine-rich repeat–containing protein 31 (LRRC31), kallikrein serine proteases, and calpain 14 (CAPN14), which have been linked to EoE.[26-28]

Although there have been significant advances in our understanding of a link between allergic inflammation and EoE, there is a paucity of data revealing the underlying pathways that regulate the epithelial BZH and DIS in patients with EoE. The DIS, also described as spongiosis, is a morphologic feature that has been identified in multiple forms of esophagitis, including lymphocytic esophagitis,[29] gastroesophageal reflux disease (GERD),[30] and EoE.[8,31] Histologic comparison between GERD and EoE suggests that DIS are significantly more intense in patients with EoE than in those with GERD.[32] Steroid therapy or an elimination diet significantly decreases DIS in patients with EoE, and this decrease is associated with improvement of patients' symptoms,[31] indicating an association between DIS and the cause of EoE. The underlying molecular pathways that drive DIS formation are currently unknown.

Recently, we performed RNA sequencing (RNAseq) on esophageal mucosal biopsy specimens from healthy control subjects and patients with active proton pump inhibitor–confirmed EoE. We identified a total of 1607 significantly dysregulated transcripts (1096 upregulated and 511 downregulated), with 66% of the gene signature being similar to the EoE transcript signature identified by means of microarray-based expression profiling.[24] We have performed Gene Ontology (GO) enrichment network analysis of the 1607 significantly dysregulated transcripts and identified dysregulation of transmembrane

transporter activity genes associated with regulation of $[pH]_i$ and acid-protective mechanisms. The most dysregulated transmembrane transporter activity gene in the EoE transcriptome was the solute carrier family 9, subfamily A, member 3 *(SLC9A3)*, which encodes sodium-hydrogen exchanger member 3 (NHE3; 33-fold increase).[33] We demonstrate a significant increase in *SLC9A3* in the esophageal epithelium in 2 independent, confirmatory patient cohorts with proton pump inhibitor–confirmed EoE. We show that the expression level of NHE3 positively correlated with the level of inflammation and the area of the DIS. IL-13 treatment of esophageal epithelial primary cells derived from patients with EoE and in a differentiated squamous esophageal epithelium model (EPC2-ALI) increased NHE3 expression and ion transport activity. Pharmacologic inhibition of NHE3 function substantially decreased the area of IL-13–induced DIS. These collective data suggest that increased expression and activity of NHE3 contribute to formation of DIS in the esophageal epithelium in patients with EoE.

METHODS

Human subjects

Healthy control subjects were defined as having no history of EoE diagnosis, 0 esophageal eosinophils per high-power field (hpf), and no evidence of esophagitis within distal esophageal biopsy specimens obtained during the same endoscopy procedure as the analyzed samples. EoE was defined as described in the recent consensus guidelines.[5] Specifically, patients needed to have 15 or more eosinophils in at least 1 hpf in an esophageal biopsy specimen, with other causes of esophageal eosinophilia excluded and without a response to acid suppression. The healthy control cohort consists of patients with a variety of nonspecific upper gastrointestinal complaints, including vomiting, loose stools, abdominal pain, and nausea who underwent endoscopy and biopsy and were demonstrated to have no histologic evidence of esophageal disease. RNAseq and validation quantitation RT-PCR (qRT-PCR) analyses and histology (eosinophils/hpf and DIS quantification) studies were performed on esophageal biopsy specimens. RNAseq and qRT-PCR analyses and histology (eosinophils/hpf and DIS) were performed on human esophageal biopsy specimens (healthy subjects, n = 6; patients with EoE, n = 10), as previously described (National Center Biotechnology Information Gene Expression Omnibus database under accession GSE58640; cohort 1).[24] The demographics of the healthy control subjects and patients with EoE are described in Fig E1 in this article's Online Repository at www.jacionline.org. The qRT-PCR and histopathologic (eosinophils/hpf) analyses were performed on a second independent cohort (healthy subjects, n = 10; patients with EoE, n = 10; cohort 2). The demographics of the patients and control subjects are described in Fig E1.

RNAseq of human biopsy specimens. Esophageal biopsy RNA was isolated from control subjects and patients with EoE with active disease by using the RNeasy kit (Qiagen, Germantown, Md), according to the manufacturer's protocol. RNA libraries were prepared by using standard Illumina protocols (TrueSeq RNA LS Sample Prep V2; Illumina, San Diego, Calif) at the Cincinnati Children's Hospital Medical Center (CCHMC) Genetic Variation and Gene Discovery Core. RNAseq acquiring 100-bp reads from paired-end libraries was performed at the Genetic Variation and Gene Discovery Core Facility at CCHMC by using the Illumina HiSeq 2500. The paired-end sequencing reads were aligned against the GRCh37 genome model by using TopHat 2.04 with Bowtie 2.03.[34,35] The separate alignments were then merged by using Cuffmerge[36] with UCSC gene models as a reference. Raw data were assessed for statistical significance by using a Welch *t* test with a Benjamini-Hochberg false discovery rate and threshold *P* value of less than .05 and a 2.0-fold cutoff filter in GeneSpring GX (Agilent Technologies, Santa Clara, Calif).

RNAseq of mature EPC2-ALI. RNA was isolated with the RNeasy kit (Qiagen), according to the manufacturer's instructions. Assessment of RNA quality was performed by using the Agilent 2100 Expert Bioanalyzer (Agilent Technologies), and only those samples with an RNA integrity number of greater than 8 were chosen for sequencing. Next-generation sequencing analyses were performed by using the CCHMC Genetic Variation and Gene Discovery Core with the Illumina HiSeq 2500. Raw data were uploaded on Biowardrobe,[37] and reads per kilobase million values were calculated. Differentially expressed genes were assessed by using DEseq2.

GO analysis. Gene set enrichment analysis and candidate gene prioritization based on molecular function were determined by using ToppGene[38] with FDR Benjamini-Hochberg correction and a *P* value cutoff of .05. Heat maps were generated by using RStudio.

Pathologic analysis

Biopsy preparation. Formalin-fixed, paraffin-embedded esophageal biopsy sections were sectioned into 5-μm slides. After removal of paraffin and serial hydration, sections were stained with hematoxylin and eosin (H&E). H&E-stained slides were then imaged with an Olympus DP-72 microscope (Olympus, New York, NY).

Quantification of the intercellular space. The intercellular space was quantified as the percentage of intercellular area of the total area of the biopsy sample by using the Image-Pro Plus software (Media Cybernetics, Rockville, Md) automated space measurement function and calculated based on the ratio of intercellular area/total tissue area.

Quantitative PCR analysis

RNA samples were extracted from esophageal biopsy specimens, cultured primary cells, or EPC2-ALI cultures by using the RNeasy kit (Qiagen), according to the manufacturer's protocol. Purified RNA (300-500 ng) was DNAse treated and reverse transcribed to cDNA by using Superscript II RNase H Reverse Transcriptase (Thermo Fisher Scientific, Rockford, Ill), according to the manufacturer's instructions. cDNA for *SLC9A3* and *18S* was quantified by using real-time PCR with TaqMan Universal Supermix with the CFX96 Real-Time PCR Detection System. Quantitative PCR analysis was performed with the Bio-Rad CFX Manager Software (version 3.1; Bio-Rad Laboratories, Hercules, Calif). Primers for *SLC9A3* and *18S* were purchased for TaqMan assay (Thermo Fisher Scientific, Waltham, Mass).

Immunofluorescence staining

For immunofluorescence (IF) staining, formalin- or paraformaldehyde-fixed, paraffin-embedded esophageal biopsy specimens or EPC2-ALI cultures were sectioned, mounted on slides, and deparaffinized with standard histologic procedures. Slides were then permeabilized in Tris-EDTA (1 mmol/L, pH 9.0) with 0.1% Tween-20, and antigen exposure was performed at 125°C for 30 seconds in a decloaking chamber by using a pressure cooker. Slides were then blocked with 10% normal donkey serum for 1 hour, followed by overnight incubation of primary antibodies diluted in 10% normal donkey serum: NHE3 (Novus, Littleton, Colo) and CK13 (Invitrogen, Carlsbad, Calif). Slides were then washed and incubated with secondary antibody at room temperature for 1 hour. Slides were mounted with Fluoromount-G (SouthernBiotech, Birmingham, Ala) mounting solution. Fluorescence imaging was performed with the Zeiss Apotome fluorescent microscope (Zeiss, Oberkochen, Germany) with NIKON elements software (Nikon, Tokyo, Japan) and ImageJ software (National Institutes of Health, Bethesda, Md).

Primary cell preparation

Distal esophageal biopsy specimens were obtained from healthy control subjects or patients with EoE who underwent routine endoscopy, suspended in 1 mL of keratinocyte serum-free media (KSFM; Invitrogen) containing supplements (human epidermal growth factor [1 ng/mL], bovine pituitary extract [50 μg/mL], and 1× penicillin/streptomycin; Invitrogen), and then placed in a 60-mm dish in 3 mL of filter-sterilized (0.2 μm) Leibovitz L-15 media (Invitrogen) containing 115 U/mL collagenase, 1.2 U/mL Dispase, and

1.25 mg/mL BSA. The biopsy specimen was mechanically dispersed by using scissors to pieces of less than 1 mm in size and then incubated at 37°C for 1 hour. The cell suspension was centrifuged at 500*g* for 5 minutes at 4°C, and the pellet was washed twice with 5 mL of supplemented KSFM. Cells were suspended in 1 mL of 0.05% trypsin/EDTA for 10 minutes at 37°C and agitated every 2 minutes. Trypsin activity was inhibited with soybean trypsin inhibitor (250 mg/L in 1× Dulbecco-PBS; 5 mL). Cells were pelleted by means of centrifugation, suspended in 1 mL of KSFM containing supplements, transferred to a 35-mm dish containing irradiated NIH 3T3 J2 fibroblasts (162,500 cells) and cultured at 37°C in a 5% CO_2 atmosphere. Medium was changed at day 5 and every other day thereafter by using KSFM containing supplements. After epithelial cells became 60% to 70% confluent, they were dispersed from the plate by using 0.05% trypsin/EDTA for 10 minutes at 37°C and agitated every 2 minutes. Trypsin digestion was inactivated by using soybean trypsin inhibitor, and cells were then passaged in KSFM containing supplements at 1 to 2 × 10^5 cells per 3 mL in a 60-mm dish.

pH_i assay

Primary esophageal epithelial cells were cultured on a ibidi μ-Slide 4 well (ibidi GmbH, Planegg, Germany) with a concentration of 25,000 cells/well. After a 24-hours equilibration period, cells were stimulated with or without 100 ng/mL recombinant human IL-13 (PeproTech, Rocky Hill, NJ) for another 48 hours. pH_i changes in these primary cells were measured with the pH-sensitive fluorescent dye BCECF AM (2′,7′-bis-[2-carboxyethyl]-5-[and-6]-carboxyfluorescein, acetoxymethyl ester) or SNARF-5F AM (SNARF-5F 5-[and-6]-carboxylic acid, acetoxymethyl ester; Invitrogen). Cells were loaded with 10 μmol/L BCECF AM or SNARF-5F AM in HCO_3^--free Ringer solution (110 mmol/L NaCl, 25 mmol/L Na-gluconate, 5 mmol/L KCl, 0.5 mmol/L $MgSO_4.7H_2O$, 1 mmol/L $CaCl_2.2H_2O$, 10 mmol/L HEPES, and 4 mmol/L glucose to pH 7.4) at 37°C for 30 minute before the experiment. Cells were washed 3 times with HCO_3^--free Ringer solution at the end of the incubation period to remove the extracellular dye. To acidify the intracellular compartment of cells and generate the necessary H^+ gradient (high $[H^+]$ inside vs low $[H^+]$ outside cell) to measure pHi recovery rate, 20 mmol/L NH_4Cl was added to the chamber after the first 5-minute recording of the baseline pH_i (Stage II). To measure the Na^+-dependent pH_i recovery rate, Na^+ was first removed from the cells by replacing the buffer with Na^+-free Ringer solution (135 mmol/L NMDG-Cl, 5 mmol/L KCl, 0.5 mmol/L $MgSO_4.7H_2O$, 1 mmol/L $CaCl_2.2H_2O$, 10 mmol/L HEPES, and 4 mmol/L glucose to pH 7.4] for 5 minutes (Stage III). The Na^+-dependent pH_i recovery rate was measured by replacing extracellular solution with HCO_3^--free Ringer solution containing 135 mmol/L Na^+ (Stage IV) and determination of the slope of the Na^+-dependent pH_i change. pH_i values are derived from the calibration curves described below. The statistical significance of the Na^+-dependent pH_i change was determined by using the Student *t* test (2-tailed).

Cells were imaged with a Nikon Spectra X inverted fluorescent microscope with the excitation wavelength of 512 nm/440 nm and emission at 535 nm to record the BCECF AM fluorescence change. Cells were imaged by using a Zeiss LSM710 LIVE DUO confocal microscope with an excitation wavelength of 488 nm and emission wavelength of 640 nm/580 nm to record the SNARF-5F AM fluorescence change. S3226 (30 μmol/L) or 0.01% dimethyl sulfoxide (DMSO; vehicle) was applied throughout the experiment to inhibit NHE3 activity. The percentage S3226-sensitive Na^+-dependent pH_i recovery rate was calculated as the recovery rate as follows:

$$(\text{DMSO-treated} - \text{S3226-treated}) * 100/\text{DMSO-treated percentage}.$$

Quantification was performed on 10 to 20 cells randomly picked in each sample, and fluorescence intensity was measured with Nikon Elements microscope imaging software or ImageJ software (National Institutes of Health, Bethesda, Md). These fluorescence intensity values were then converted into pH values per calibration curve. A calibration curve was generated at the end of each experiment; BCECF AM or SNARF-5F AM intensity was calibrated against pH_i when cells were exposed to the K^+/H^+ ionophore nigericin (10 μmol/L) and valinomycin (10 μmol/L; Invitrogen) in high-K^+ solution at 4 different pH values. High-K^+ solution (20 mmol/L NaCl, 130 mmol/L KCl, 1 mmol/L $MgCl_2$, 1 mmol/L $CaCl_2.2H_2O$, and 5 mmol/L HEPES) was prepared and titrated to a pH ranging from 6.5 to 7.9. Fitting was performed with GraphPad Prism software (GraphPad Software, La Jolla, Calif).

EPC2-ALI culture

hTERT-EPC2 cells (hTERT-immortalized human esophageal keratinocytes) were a kind gift from Dr Anil Rustgi (University of Pennsylvania, Philadelphia, Pa), as previously described.[39] The air-liquid interface (ALI) culture system was previously described and characterized together with EPC2 cells.[28] EPC2 cells were grown to fully submerge on 0.4-μm pore size, permeable transwell inserts (Corning, Corning, NY) in KSFM (Life Technologies, Carlsbad, Calif). First, at day 0, cells were seeded on a permeable membrane and grown to single submerged layer after 3 days. Second, cells were then shifted to medium containing high $[Ca^{2+}]$ to induce tight junction formation ($[Ca^{2+}]$ = 1.8 mmol/L). Third, on day 7, media were removed from the top chamber to induce differentiation and epithelial stratification at the ALI. Fourth, at day 12 (5 days after ALI), cells were treated with vehicle or cytokine (IL-13) in the presence and absence of SLC9A3 inhibitor S3226 (30 μmol/L),[40] as described in the figure legends.

Lentiviral transduction

EPC2 cells at 60% to 70% confluence were transduced with lentiviral particles containing Mission STAT6 short hairpin RNA (shRNA) TRC 0000019409 shRNA or Mission STAT3 (TRCN0000329887) shRNA (Sigma, St Louis, Mo) or Mission nontarget control shRNA (Sigma). All 3 shRNA lentiviruses were generated by the CCHMC Viral Core by using a 4-plasmid packaging system. Lentiviral particles were incubated with EPC2 cells for 6 hours at a multiplicity of infection of 0.5 to 10 for signal transducer and activator of transcription (STAT) 3 or control shRNA. For STAT6 shRNA, 10 to 50 μL of viral particles were added to the cells. All viral particles were added in the presence of 5 μg/mL Hexadimethrine bromide (Polybrene; Sigma).

During the first hour of incubation, cells were spun down at 1000*g* for 1 hour at room temperature. Six hours After transduction, cells were put in fresh KSFM, and 24 hours later, medium containing 1 μg/mL Puromycin (Thermo Fisher Scientific) was used for selection. Cells were grown under selective pressure and cultured as regular EPC2 cells. Stable knockdown of STAT6 and STAT3 in EPC2-ALI cultures was evaluated by using Western blotting. Results indicated an 80% reduction in STAT6 and 90% reduction in STAT3 expression, relatively, compared with that seen in empty control transduced cells.

Western blot

EPC2-ALI cultures were lysed by using protein lysis buffer (10% glycerol, 20 mmol/L Tris HCl [pH 7], 137 mmol/L NaCl, 2 mmol/L EDTA, and 1% NP-40 in H_2O) supplemented with Halt protease inhibitor cocktail (Thermo Fisher Scientific). Proteins were then quantified with the bicinchoninic acid assay, and 20 μg of protein extracted together with protein-reducing buffer was loaded and separated on a 4% to 12% Bis-Tris gel and transferred to a nitrocellulose membrane (Life Technologies). Antibodies of NHE3 and α-actin were used for protein detection. The IRDye 800 CW goat anti-rabbit IgG (H+L; LI-COR, Lincoln, Neb) was used as the secondary antibody for detection. Western blot quantification was performed with Image Studio Lite (LI-COR).

pH-STAT assay

Acid secretion by confluent epithelium was quantitated by using pH-STAT (TIM856; Radiometer Analytical, Loveland, Colo) connected to an Ussing chamber system, as previously described.[41] EPC2-ALI cultures were mounted to an Ussing chamber containing unbuffered Ringer solution (145 mmol/L NaCl, 2 mmol/L KCl, 1 mmol/L $MgCl_2$, 2 mmol/L $CaCl_2$, and 5 mmol/L

glucose) and gassed with 99.5% oxygen. Both the pH electrode and titrating burette are placed in the apical side chamber.

Extracellular pH was measured for 10 minutes or until a stable pH was achieved (<0.002 pH unit change/min) to measure the equilibrium extracellular pH without any titration. After the equilibrium period and extracellular pH measurements were obtained, the pH of the mucosal side was adjusted by titration to a set alkaline pH (pH 7.6) to create the electrochemical driving force for acid secretion. The titration rate (ie, the amount of alkaline injected by the machine to neutralize the acid secreted by EPC2-ALI culture to maintain the set pH) was used to measure the acid secretion rate.

Histologic analysis for EPC2-ALI cultures

EPC2-ALI cultures were treated as indicated in experiments and then fixed on transwell supports with 4% paraformaldehyde for 1 hour at room temperature. Fixed membranes underwent a series of dehydration steps, cleared in Histoclear solution, embedded in paraffin, and sectioned into 5-μm slides. The slides were stained by using H&E staining and imaged with an Olympus DP-72 microscope (Olympus).

Electron microscopy

EPC2-ALI cultures were treated as indicated in experiments, fixed with 3% glutaraldehyde, and submitted to the CCHMC Pathology Research Core for processing, sectioning, and transmission electron microscopy by using a Hitachi model H-7650 electron microscope at 80 kV with the AMT-600 image capture engine software.

Statistical analysis

The statistical significance of EPC2-ALI samples was established by using an unpaired *t* test (2-tailed) or 2-way ANOVA if there was more than 1 variable. For nonnormally distributed data from patients' biopsy specimens and primary cells derived from patients' biopsy specimens, the Mann-Whitney test was used, and correlation analyses were assessed with a Spearman correlation test. Graphing and statistical analyses were performed with GraphPad Prism (7.02; GraphPad Software).

RESULTS

Transmembrane transporter *SLC9A3*/NHE3 was specifically upregulated and correlated with eosinophil counts and DIS in patients with EoE

To begin to determine the potential involvement of transmembrane transporter activity in the histopathologic alterations of the esophageal epithelium in patients with EoE, we applied GO enrichment analysis of the 1607 differentially expressed RNA transcripts identified by means of RNAseq analyses of pediatric biopsy specimens from healthy control subjects and patients with EoE.[24] GO analysis revealed 50 individual GO nodes significantly dysregulated in the EoE transcriptome based on functional annotations and protein interaction networks (FDR-corrected $P < .05$, see Fig E2 in this article's Online Repository at www.jacionline.org). Of these GO nodes, 5 were related to transmembrane transporter activity (Fig 1, *A*). A combinatory comparison of all 62 genes within these 5 GO nodes revealed that the most upregulated transmembrane transporter activity gene was *SLC9A3*, which encodes for NHE3 (Fig 1, *B*). *SLC9A3* was induced 33-fold in patients with EoE compared with healthy control subjects (Fig 1, *C*). In contrast, expression of other members of the SLC9 family, including the ubiquitously expressed sodium-proton exchanger solute carrier family 9, subfamily A, member 1 (SLC9A1), also referred to as sodium-hydrogen exchanger family member 1, was not dramatically different between patients with EoE and healthy control subjects (Fig 1, *D*). Correlation analyses revealed a positive correlation between the level of peak distal esophageal eosinophil count and *SLC9A3* expression ($r = 0.7167$, $P < .05$; Fig 1, *E*). Notably, this was specific to *SLC9A3* because we did not observe any correlation with *SLC9A1* ($r = 0.3201$, $P > .05$; Fig 1, *E*), revealing a specific link between *SLC9A3* expression and disease severity in patients with EoE.

To confirm these observations, we examined a second independent pediatric cohort (healthy control subjects, n = 10; patients with active EoE, n = 10), for which we had paired RNA and histologic biopsy samples from the same day of endoscopy. Consistent with our RNAseq analyses, quantitative PCR analyses revealed significant *SLC9A3* overexpression in the pediatric EoE cohort (Fig 1, *F*). Furthermore, we observed a positive Pearson correlation between *SLC9A3* expression level and distal peak esophageal eosinophil numbers ($r = 0.9172$, $P < .0001$; Fig 1, *G*).

We next performed IF analyses to determine the cellular and spatial expression of NHE3 in esophageal biopsy specimens from healthy control subjects and patients with EoE. Consistent with our RNAseq and PCR analyses, we observed very little expression of NHE3 in healthy esophageal epithelium (Fig 1, *H*, upper panel). The positive staining observed was restricted to the $CK13^-$ single-cell basal esophageal epithelial layer (Fig 1, *H*, upper panel). In patients with EoE, NHE3 protein expression was remarkably increased, localized to the esophageal basal cell layer, and expanded into the $CK13^+$ suprabasal layer (Fig 1, *H*, lower panel). Localization of NHE3 to the suprabasal zone, an area associated with DIS formation, led us to examine the relationship between *SLC9A3* expression and DIS in esophageal biopsy specimens from patients with EoE. Notably, *SLC9A3*, but not *SLC9A1*, expression positively correlated with the percentage of DIS area in patients with EoE ($r = 0.8095$, $P < .05$; Fig 1, *I*). These cumulative data indicate specific upregulation of *SLC9A3*/NHE3 in the suprabasal layer of the esophageal epithelium in patients with EoE and that *SLC9A3* expression correlates with esophageal eosinophilic inflammation and DIS.

Increased NHE3 function in IL-13–stimulated primary esophageal epithelial cells

The epithelial sodium-proton exchanger NHE3 is expressed predominantly in the apical membrane of the epithelium and is the principal mechanism for electroneutral exchange of (Apical → Baso) Na^+ and (Baso → Apical) H^+ and plays an important role in maintenance of pH_i and regulation of cell volume.[42] Given IL-13's known role in upregulating the EoE transcriptome[18] and that the humanized anti–IL-13 mAb QAX576 has been shown to modulate expression of an anion transport activity node,[25] we examined the effect of IL-13 exposure on *SLC9A3* expression in primary esophageal epithelial cells. We demonstrate upregulation of *SLC9A3* expression in primary esophageal epithelial cells after IL-13 stimulation (Fig 2, *A*).

To determine whether increased *SLC9A3* expression was associated with altered NHE3 activity, we examined the effect of IL-13 exposure on pH_i in primary esophageal epithelial cells. Notably, increased *SLC9A3* expression coincided with a significant increase in baseline pH_i (Fig 2, *B*) and Na^+-dependent pH_i recovery rate (Fig 2, *C* and *D*), supporting an overall increase in Na^+/H^+ exchange activity. Notably, the recovery rate correlated positively with *SLC9A3* expression in primary esophageal

A

GO ID	GO name	p Value	Genes from Input	Genes in annotation
GO: 0046943	Carboxylic acid transmembrane transporter activity	2.16E-05	26	141
GO: 0008028	Monocarboxylic acid transmembrane transporter activity	2.64E-05	13	46
GO: 0008509	Anion transmembrane transporter activity	0.0003175	40	297
GO: 0022804	Active transmembrane transporter activity	0.0004732	46	363
GO: 0042887	Amide transmembrane transporter activity	0.0004741	7	20

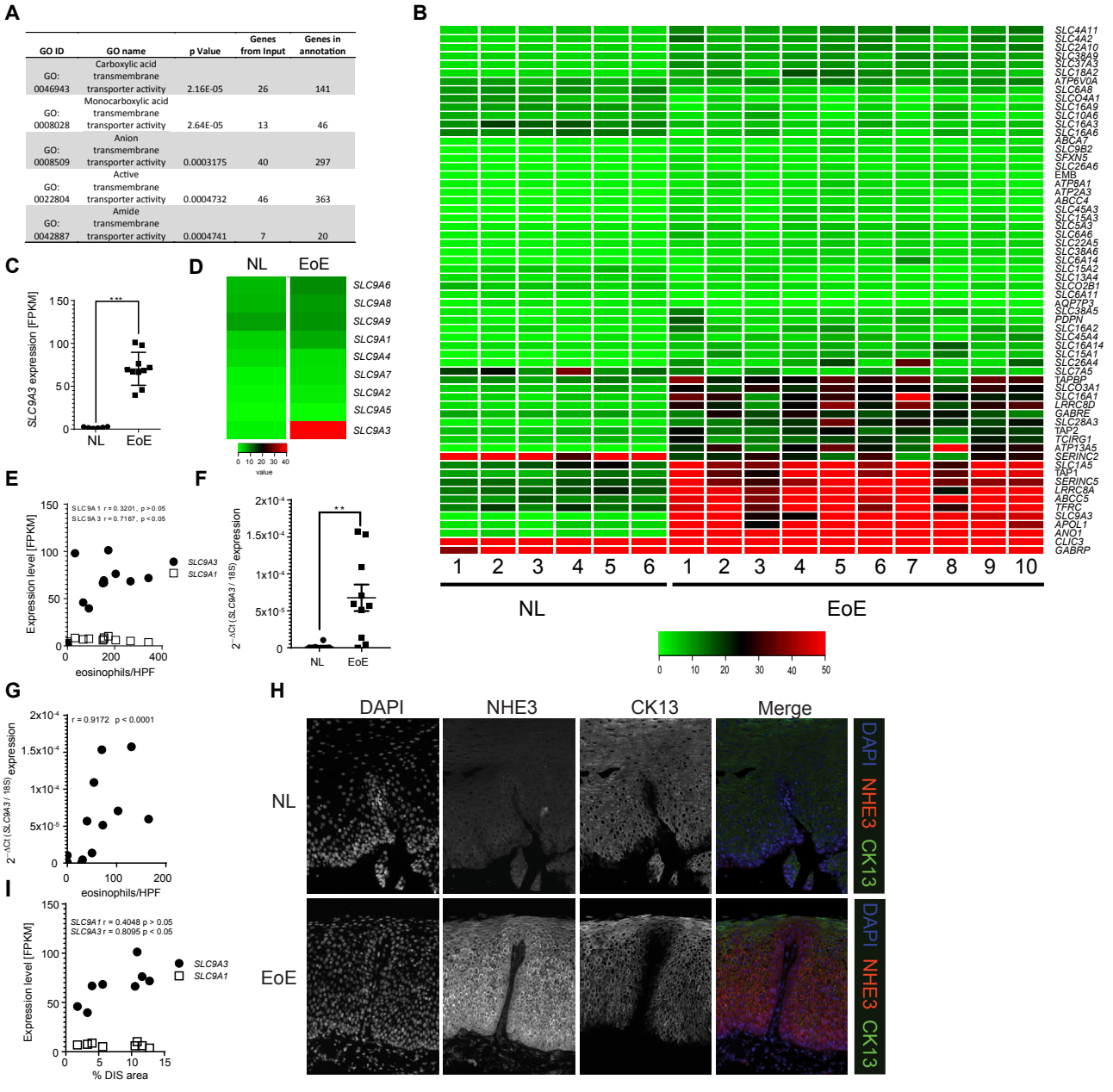

FIG 1. *SLC9A3* is the most upregulated transmembrane transporter activity gene in the EoE transcriptome, and its expression correlates with EoE severity and DIS. **A,** GO nodes associated with transmembrane transporter activity–related genes identified by using GO enrichment analysis of 1610 dysregulated genes from RNAseq. **B,** Heat map depicting the expression level of 62 individual genes within the transmembrane transporter activity GO nodes. **C** and **D,** Individual fragment per kilobase million (FPKM) values of *SLC9A3* (Fig 1, *C*) and heat map depicting expression level of *SLC9A1-9* (Fig 1, *D*). **E,** Correlation analysis of *SLC9A3* or *SLC9A1* expression and matched peak distal eosinophils/hpf in esophageal biopsy specimens (healthy control subjects *[NL]*, 6; patients with EoE = 10). **F** and **G,** Quantitative PCR analysis of *SLC9A3* expression (Fig 1, *F*) and Spearman correlation relating *SLC9A3* expression (Fig 1, *G*) and eosinophils/hpf in an independent validation cohort (healthy control subjects, 10; patients with EoE, 10). **H,** IF staining of esophageal biopsy sections from healthy control subjects *(top panel)* and patients with EoE *(lower panel)*. NHE3 (red), CK13 (green), and nuclei (4′-6-diamidino-2-phenylindole dihydrochloride *[DAPI]*, blue) are shown. Images are representative of 7 patients per group. Magnification ×40. **I,** Spearman correlation between *SLC9A3* or *SLC9A1* expression and percentage of DIS in esophageal biopsy specimens from patients with active EoE (n = 8). Fig 1, *C* and *F*, Data are represented as average ± SEM. Fig 1, *E*, *G*, and *I*, Data are presented as relative expression over *18S*. Fig 1, *C*, *E-G*, and *I*, Individual symbols represent individual patients. $^{**}P < .01$ and $^{***}P < .001$.

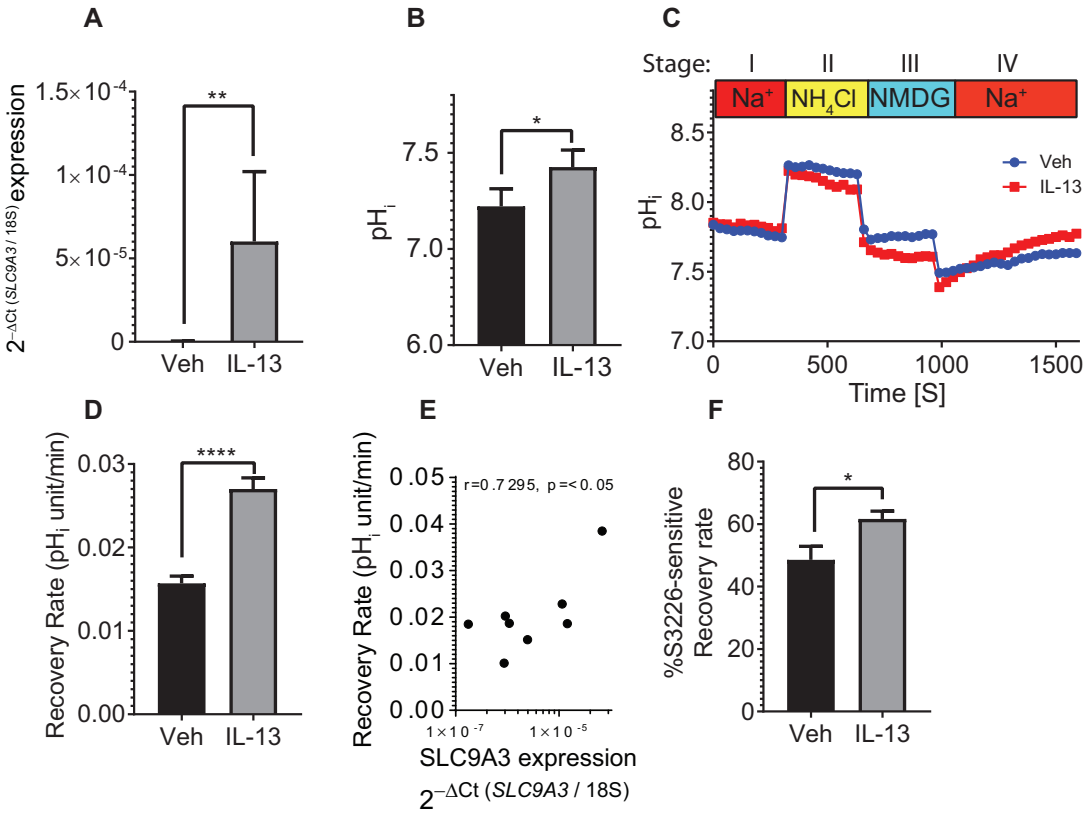

FIG 2. Increased *SLC9A3*/NHE3 expression and activity in primary esophageal epithelial cells derived from EoE biopsy specimens in response to IL-13. **A,** Quantitative PCR analysis of *SLC9A3*. **B,** Baseline pH_i. **C,** Representative curves of pH_i change over time. **D,** Na^+-dependent pH_i recovery rate of cells derived from biopsy specimens of patients with active EoE (n = 6) treated with vehicle *(Veh)* or IL-13. **E,** Spearman correlation analysis comparing the *SLC9A3* expression level and Na^+-dependent pH_i recovery rate (n = 5 individual patients stimulated with vehicle and IL-13). **F,** Percentage of S3226-sensitive Na^+-dependent intracellular recovery rate in cells treated with vehicle or IL-13. See the Methods section for the detailed protocol. Fig 2, *B*, Data represent the average ± SEM pH_i of cells from patients with active EoE (n = 8). Fig 2, *C*, Each data point represents the average value of 40 individual cells from 2 individual experiments. Data points represent the average value of 120 individual cells from 6 different patients with active EoE (Fig 2, *D*) and 50 individual cells from 5 different patients with active EoE (Fig 2, *F*). Fig 2, *A, B, D,* and *F,* Data are represented as average ± SEM. $*P < .05$, $**P < .01$, and $****P < .0001$.

epithelial cells ($r = 0.9503$, $P < .01$; Fig 2, *E*), suggesting that the increase in pH_i recovery rate in IL-13–treated primary esophageal epithelial cells is predominantly caused by increased NHE3 expression. Addition of the NHE3-specific inhibitor S3226 (30 μmol/L) confirmed that the IL-13–induced increase in Na^+-dependent pH_i recovery rate was mediated predominantly by NHE3 (Fig 2, *F*).

IL-13 induces an EoE-like transcriptome, including increased transmembrane transporter activity and *SLC9A3* overexpression, in an *in vitro*, matured, esophageal epithelial model system

To define the involvement of *SLC9A3*/NHE3 in regulation of pH_i and DIS formation in a mature esophageal epithelial model system, we adapted an *in vitro* model developed from keratinocyte esophageal epithelial cells (EPC2) grown at the ALI.[28] EPC2s were grown under submerged conditions in low-calcium media (0.09 mmol/L, days 0-3), changed to high-calcium media (1.8 mmol/L, days 3-7), and then exposed to the ALI for 5 days in the presence of high calcium levels (1.8 mmol/L, days 7-12) to induce differentiation and formation of a mature stratified epithelium (Fig 3, *A*). After maturation, EPC2-ALI cultures were stimulated with vehicle or IL-13, and RNAseq analyses were performed (days 12-14; Fig 3, *A*). We show that IL-13 significantly dysregulated a total of 572 genes ($P < .05$, fold change > 2.0); notably, many of the most highly dysregulated genes included inflammatory genes associated with EoE, including *CCL26* (7-fold), *TNFAIP6* (9-fold), *CDH26* (3-fold), and *CAPN14* (5-fold), and also gene families located in the epidermal differentiation cluster on chromosome 1q21 (eg, *IVL*, *LOR*, *S100A4*, and *S100A6*; Fig 3, *B*, and see Table E1 in this article's Online Repository at www.jacionline.org). Consistent with these findings, comparative analyses of the IL-13–induced transcriptome changes in EPC2-ALI cultures with that of the EoE-specific transcriptome revealed significant overlap with the EoE-specific transcriptome ($P < .0001$; Fig 3, *B*). GO analysis based on the biological process on IL-13–dysregulated genes revealed the most significant 15 individual GO biological process nodes associated with keratinization, epidermis development, skin development, keratinocyte differentiation, epidermal cell differentiation, and

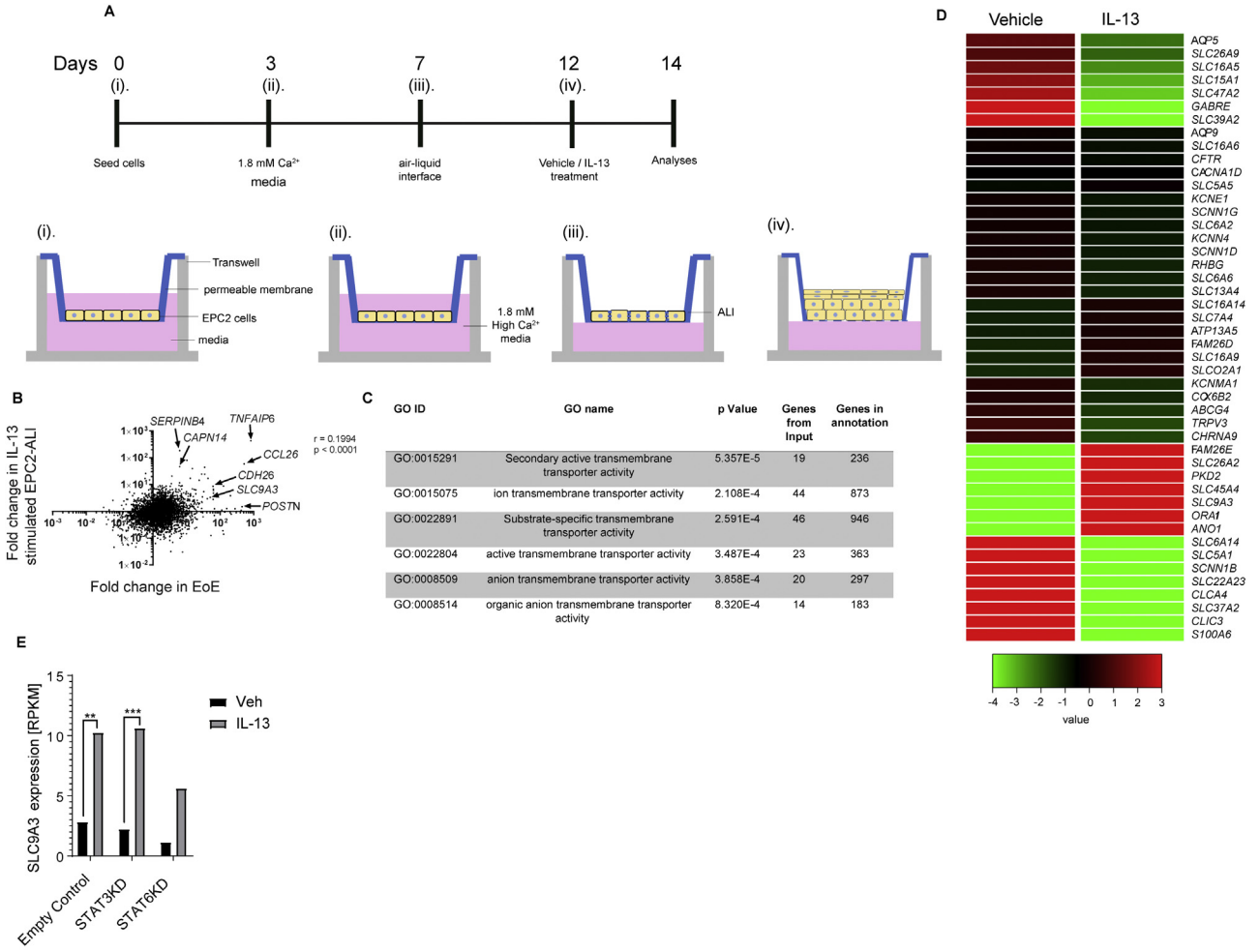

FIG 3. Mature stratified squamous esophageal epithelial model using an EPC-ALI culture system. **A,** Schematic diagram of esophageal epithelium ALI (EPC2-ALI) differentiation protocol (see the Methods section). **B,** Gene expression change of IL-13–stimulated EPC2-ALI versus nontreated EPC2-ALI cultures compared with that of patients with active EoE versus healthy control subjects. Fold changes were calculated from RNAseq of EPC2-ALI cultures and patient samples. Spearman correlation analysis was applied to analyze these 23,660 genes. **C,** GO analysis of 572 genes that were significantly dysregulated by IL-13 treatment of EPC2-ALI cultures (fold change > 2, $P < .05$) identified 6 GO nodes related to transmembrane transporter activity. **D,** Heat map depicting expression level of 46 individual genes within the transmembrane transporter activity GO nodes that are significantly dysregulated in EPC2-ALI cultures after IL-13 stimulation. **E,** Reads per kilobase million values indicating *SLC9A3* expression level in empty control *(CTRL)*, *STAT3* lentiviral knockdown *(STAT3KD)*, and *STAT6* lentiviral knockdown *(STAT6KD)* EPC2-ALI cultures treated with vehicle *(Veh)* or IL-13 (n = 3 per treatment). **Adjusted $P < .01$ and ***adjusted $P < .001$.

inflammatory response and GO pathways associated with formation of the cornified envelope, keratinization, and IL-4 and IL-13 signaling (FDR-corrected $P < .05$; see Table E2 in this article's Online Repository at www.jacionline.org).

To examine the effect of IL-13 on transmembrane transporter activity, we performed GO analysis based on the molecular function of the 572 genes and identified 6 nodes dysregulated significantly and related to transmembrane transport activity (FDR-corrected $P < .05$; Fig 3, *C*). Of the 28 differentially expressed transmembrane transport activity genes in these 6 GO nodes, *SLC9A3* was one of the most highly upregulated genes (Fig 3, *D*).

IL-13 is known to signal through the Janus kinase/STAT pathway, in particular through a STAT3- and STAT6-dependent signaling pathway.[43] To determine the involvement of STAT3 and STAT6 in IL-13 induction of SLC9A3, we examined *SLC9A3* mRNA expression in *STAT3 and STAT6* shRNA–transduced EPC2-ALI cultures after IL-13 stimulation. Notably, STAT3 knockdown in EPC2-ALI cultures caused no significant reduction in IL-13–induced *SLC9A3* expression compared with control shRNA–transduced EPC2-ALI cultures (Fig 3, *E*). In contrast, *STAT6* knockdown in EPC2-ALI cultures significantly ablated IL-13–induced *SLC9A3* expression (50% reduction), suggesting that IL-13–induced STAT6 signaling is important for *SLC9A3* expression in EPC2-ALI cultures (Fig 3, *E*). These studies demonstrate that IL-13 induces *SLC9A3* expression in EPC2-ALI cells in part through a STAT6-dependent mechanism.

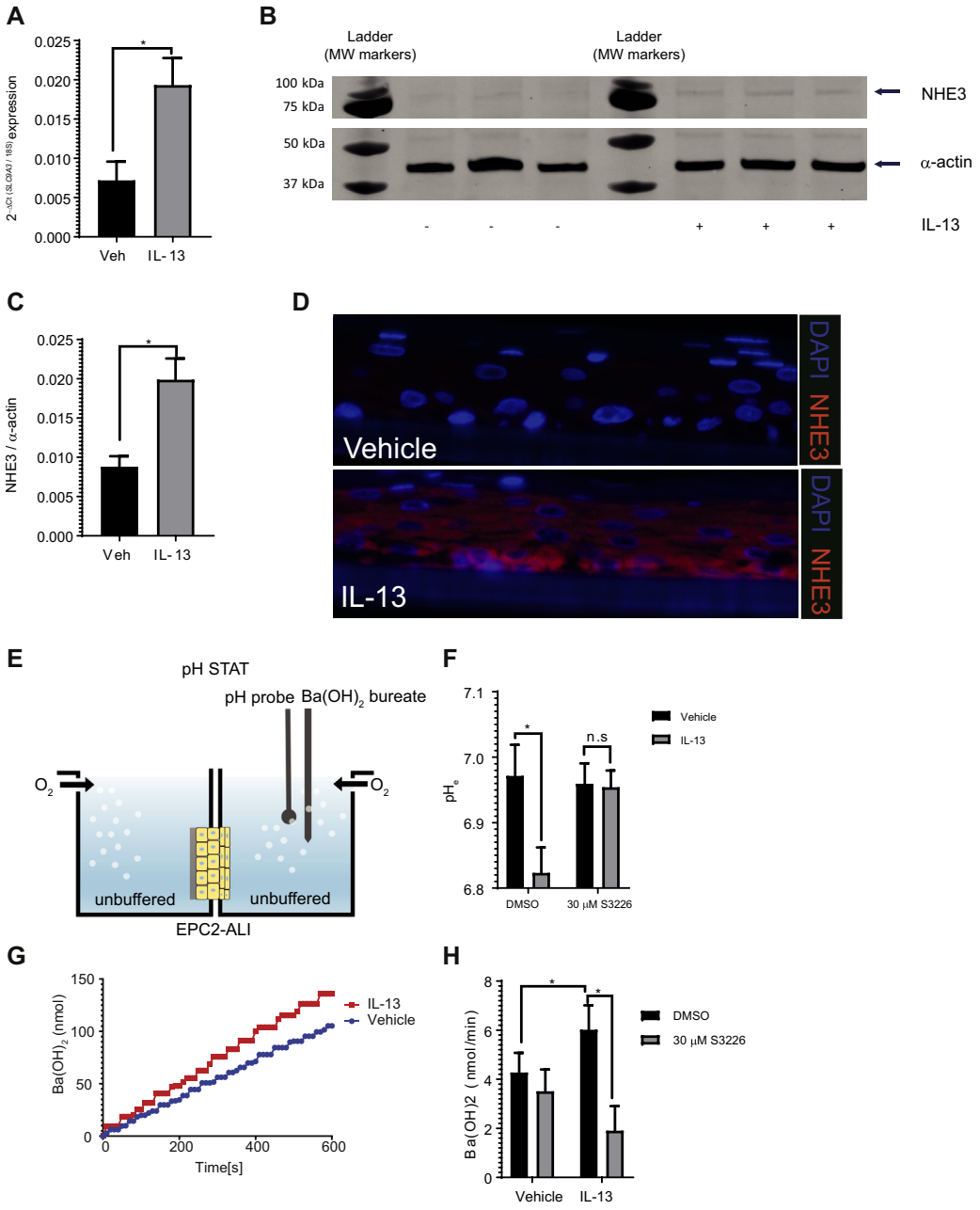

FIG 4. Increased *SLC9A3*/NHE3 expression and activity in IL-13–stimulated EPC2-ALI multicell layer cultures. **A-C,** Quantitative PCR (Fig 4, *A*), Western blot analysis (Fig 4, *B*), and Western blot quantification (Fig 4, *C*) of *SLC9A3*/NHE3 expression in EPC2-ALI cultures after a 72-hour treatment with vehicle *(Veh)* or IL-13 (100 ng/mL). *Ct,* Cycle threshold; *MW,* molecular weight. **D,** IF staining of vehicle-stimulated *(top panel)* or IL-13–stimulated *(lower panel)* EPC2-ALI cultures. NHE3 (red) and nuclei (blue) are shown. Images are presentative of 3 samples per group. Magnification ×400. **E,** Schematic view of pH-STAT assay. See the Methods section for a detailed protocol. **F,** Baseline extracellular pH (pH_e) of EPC2-ALI multicell layer cultures treated with vehicle or IL-13 for 72 hours. DMSO (0.1%) or S3226 (30 μmol/L) was added to both sides of the chamber during the experiment (n = 6-11 samples per group from 5 individual experiments). **G** and **H,** Amount of $Ba(OH)_2$ injection over time (Fig 4, *G*) and $Ba(OH)_2$ injection rate (Fig 4, *H*) measured for EPC2-ALI multicell layer cultures treated with vehicle or IL-13 for 72 hours. DMSO (0.1%) or S3226 (30 μmol/L) is added to both sides of the chamber during experiment (n = 6-11 samples per group from 5 individual experiments). Fig 4, *A, C, F,* and *H,* Data are represented as average ± SEM. *$P < .05$. *n.s.*, Not significant.

IL-13–induced NHE3 expression and function in differentiated esophageal epithelial cells

Using this mature EPC2-ALI model system, we show that IL-13 stimulation of EPC2-ALI multicell layer induced an increase in *SLC9A3* mRNA (Fig 4, *A*) and NHE3 protein (Fig 4, *B* and *C*) expression. IF analyses revealed that NHE3 was barely expressed in vehicle-treated EPC2-ALI multicell layer (Fig 4, *D*, top panel). In contrast, we observed a significant increase in NHE3 expression

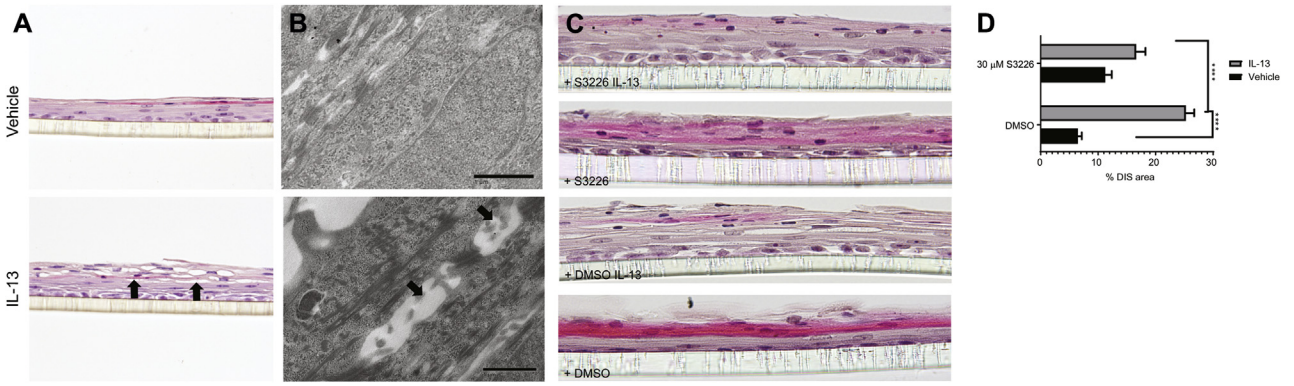

FIG 5. Blockade of NHE3 protected EPC2-ALI multicell layer cultures from IL-13–induced DIS. **A** and **B,** H&E staining (Fig 5, *A*) and electron microscopy (Fig 5, *B*) of EPC2-ALI multicell layer cultures stimulated with vehicle or IL-13 (100 ng/mL) for 72 hours and showing DIS *(black arrows)* in only IL-13–treated cells. **C,** H&E staining of EPC2-ALI multicell layer cultures stimulated with vehicle or IL-13 (100 ng/mL) in the presence and absence of S3226 (30 μmol/L) for 72 hours. **D,** DIS formation (percentage of total area) was quantitated by using morphometric analyses and expressed as the mean ± SEM (n = 3 independent experiments). ****$P < .0001$. Magnification: Fig 5, *A*, ×200; Fig 5, *B*, ×5000; and Fig 5, *C*, ×300.

in EPC2-ALI multicell layer following IL-13 exposure; comparable with what we observed in biopsy samples from patients with EoE. IF analyses revealed that NHE3 was localized predominantly to the basal and suprabasal layer of the epithelium in IL-13–treated EPC2-ALI cultures (Fig 4, *D*, lower panel).

To examine NHE3 function in mature EPC2-ALI cultures, we measured proton secretion rates in an Ussing chamber system fitted with pH-STAT (Fig 4, *E*). We show that IL-13 stimulation reduced extracellular pH compared with vehicle-treated control values (extracellular pH [pH_e]: 6.82 vs 6.97, respectively; $P < .05$), indicating altered acid-base transport. Notably, the reduction in extracellular pH was abrogated with exposure to the specific NHE3 inhibitor S3226 (Fig 4, *F*), indicating NHE3-dependent proton extrusion. To measure the rate of acid extrusion by the mature EPC2-ALI, the buffer on the apical side was adjusted to an alkaline pH (pH 7.6; $Ba[OH]_2$) to generate the electrochemical gradient necessary to stimulate acid secretion, and the amount of alkali $Ba(OH)_2$ required to maintain this condition (pH 7.6) was continuously monitored with pH-STAT (Fig 4, *G*). We show that IL-13 stimulation of mature EPC2-ALI multicell layer led to increased $Ba(OH)_2$ injection to counterbalance H^+ secretion from the tissue and maintain a pH of 7.6 (Fig 4, *G*).

S3226 was added to the apical buffer to determine the involvement of NHE3 in apical acid secretion function in the mature EPC2-ALI cultures. Notably, the acid-secretion rate in IL-13–stimulated mature EPC2-ALI multicell layer was significantly abrogated with S3226, indicating NHE3-dependent secretion (Fig 4, *H*). These observations indicate an IL-13–induced increase in NHE3-dependent acid secretion in EPC2-ALI cultures.

Increased *SLC9A3* expression and activity is linked to DIS formation

Given the observed association between NHE3 and acid secretion in EPC2-ALI cultures and the correlation between *SLC9A3* expression and DIS formation in esophageal biopsy samples from patients with EoE (Figs 1, *I*, and 4, *H*, respectively), we examined the relationship between NHE3 function and DIS formation in a mature EPC2-ALI multicell layer. IL-13 stimulation of a EPC2-ALI multicell layer induced DIS formation within the basal and suprabasal layer of EPC2-ALI cells, as evidenced by spaces between cells (Fig 5, *A*). Electron microscopy analyses revealed alteration in the intercellular junctional structures of esophageal cells, with the appearance of expanded or dilated intercellular areas (Fig 5, *B*; *black arrows*). Notably, the DIS are sealed by lateral membranes that are of close apposition and tethered by intercellular junctional proteins, such as desmosomes (Fig 5, *B*).

To determine the requirement of NHE3 activity in DIS formation, we stimulated EPC-ALI multicell layer with IL-13 in the presence of the NHE3 inhibitor S3226 (Fig 5, *C* and *D*). Notably, we show that the IL-13–induced DIS within the suprabasal layer in EPC2-ALI cells were diminished in the presence of S3226 (Fig 5, *C* and *D*). Collectively, we concluded that NHE3 has an important role in IL-13–induced DIS formation in esophageal cells.

DISCUSSION

EoE is characterized by histopathologic manifestations, including BZH and DIS. The underlying molecular processes that drive these pathologic manifestations remain largely unexplored. Here we demonstrate (1) dysregulation of transmembrane transporter activity gene networks in esophageal biopsy specimens from patients with EoE; (2) increased expression of the Na^+-H^+ exchanger *SLC9A3*/NHE3 in esophageal biopsy specimens from patients with EoE and positive correlation of this increased expression with DIS area and eosinophil infiltration; (3) increased *SLC9A3* expression and NHE3 activity in primary esophageal epithelial cells and in response to IL-13 stimulation in a mature EPC2-ALI model system; and (4) reduction of IL-13–induced DIS formation in EPC2-ALI cells by pharmacologic antagonism of NHE3 activity. Collectively, we have identified a role for *SLC9A3*/NHE3 in IL-13–induced DIS formation in the esophageal epithelium and provide evidence for involvement of this pathway in the histopathologic manifestations of EoE.

The cytokine IL-13 has an important role in driving the underlying allergic inflammatory cascade and histopathologic

features of EoE.[22-24] This notion is supported by observations that stimulating esophageal cells with IL-13 leads to a transcript signature that partially overlaps the esophageal EoE transcriptome.[18] Furthermore, although the primary outcome of a greater than 75% decrease in peak eosinophil counts at week 12 was not met, treating patients with EoE with anti–IL-13 (QAX576) reduced intraepithelial esophageal eosinophil counts and led to improvement in the EoE transcriptome and clinical symptom, such as dysphagia, in adults with EoE.[25] Our observation of increased *SLC9A3* expression in tissue samples from patients with EoE and in both primary esophageal epithelial and EPC2-ALI cultures following IL-13 stimulation was surprising given that *SLC9A3*/NHE3 expression and function are predominantly associated with induction of T_H1 proinflammatory cytokines, including IFN-γ and TNF.[44] IFN-γ and TNF are thought to modulate *SLC9A3* expression through protein kinase A–mediated phosphorylation of Sp1 and Sp3 transcription factors.[44] TNF has also been shown to alter NHE3 activity by stimulating protein kinase Cα–dependent internalization of NHE3.[45] Stimulation of EPC2-ALI cultures with other pro–type 2 cytokines, such as IL-25 and IL-33, did not lead to induction of *SLC9A3*/NHE3 mRNA expression (results not shown). Notably, a recent study in kidney and intestinal epithelial cells (Caco-2) reported a STAT3-dependent increase in *SLC9A3* expression through the recruitment of transcriptional factor Sp1 and Sp3.[46] IL-13 is known to signal through the Janus kinase/STAT pathway, in particular through a STAT3- and STAT6-dependent signaling pathway.[43] We reveal that STAT6 signaling plays a significant role in IL-13–induced *SLC9A3* expression in EPC2-ALI cultures. Examining the *SLC9A3* promoter did not reveal the presence of STAT6 binding IFN-γ activation site (GAS) elements (results not shown), suggesting that STAT6 might indirectly modulate *SLC9A3* expression. Notably, there are recent reports of IL-13–induced, STAT6-dependent activation of early growth response gene 1 (EGR1) signaling pathways in patients with EoE,[47,48] and previous studies in intestinal epithelial cells have revealed that overexpression of EGR1 promotes *SLC9A3*/NHE3 expression and activity.[49] We are currently further pursuing the molecular basis of IL-13 transcriptional regulation of *SLC9A3* expression.

SLC9A3, as a member of the Na^+/H^+ exchanger family, drives Na^+-dependent extrusion of H^+ and is primarily involved in the regulation of pH_i and acid-protective mechanisms.[50-53] A consequence of Na^+-dependent acid extrusion in a multilayered stratified epithelium, such as the esophageal epithelium, is acidification of the intercellular spaces.[54] In well-perfused tissues, where there are short diffusion distances and good cell-to-capillary diffusive coupling, the acid is rapidly buffered by phosphates, proteins, and HCO_3^-.[55] However, in stratified epithelium that is undergoing rapid and sustained cellular proliferation, the diffusion distances are increased, leading to often-inadequate capillary perfusion, which limits the capacity of the intercellular acid-protective mechanisms and neutralization of the acidified intercellular spaces. The accumulation of acid [H^+] in the intercellular spaces permits formation of an electrochemical gradient and ion diffusion, creating an osmotic force for water flux and dilation of the intercellular spaces.[56,57] In patients with EoE, there is significant esophageal epithelial basal zone expansion, and the basal cell layer can exceed 15% of the total epithelial thickness.[58] We speculate that the esophageal proliferative response and the thickening of the suprabasal layer of the esophageal epithelium in patients with EoE increases the diffusion distances, thus causing the intercellular acid-protective mechanisms to become inefficacious leading to DIS.

Consistent with the concept of esophageal epithelial intercellular acid as a primary driver for DIS in EoE, luminal acid has been shown to drive acidification of the intercellular spaces and DIS in patients with nonerosive reflux disease.[55-57,59] Furthermore, in support of this concept, a recent study reports a strong positive correlation between BZH and DIS ($r^2 \geq 0.67$) in both proximal and distal biopsy samples from pediatric patients with EoE.[60] Interestingly, the increased esophageal intercellular acid in nonerosive reflux disease is thought to activate afferent neurons (nociceptors) within the esophageal epithelium, leading to development of heartburn.[59,61] Intriguingly, although not common, EoE is also associated with the development of heartburn.[4]

SLC9A3's role in the regulation of pH_i might not simply be in response to dysregulation of pH_i but also in part fulfilling a larger role in regulation of esophageal epithelial proliferation. Moreover, intracellular pH plays an important role in many cellular functions, including proliferation[62] and apoptosis.[63] In tumor cells pH_i is often increased compared with that in normal cells, and it is thought that the alkaline pH_i provides an optimal environment for DNA synthesis relative to enzyme function.[64] Consistent with this, growth factors, such as epidermal growth factor and platelet-derived growth factor, stimulate a rapid increase in pH_i, which is a critical requirement for entry of mitogen-stimulated quiescent cells into the S phase of the cell cycle.[65,66] Experimental studies have identified an important role for NHE family members in the growth factor–induced increase in pH_i and cellular proliferation.[67,68] For example, pharmacologic abrogation of Na^+-dependent extrusion of H^+ and increase in pH_i in growth factor–stimulated mouse bone marrow–derived macrophage inhibited DNA synthesis and prevented the progression into the S phase.[67] Furthermore, the rapid and transient mitogen-induced increase in sodium-hydrogen exchanger member 1 (NHE1) activity and pH_i during G_2/M entry and transition is ablated in NHE1 mutant fibroblasts.[68] Notably, increasing the pH_i in the absence of NHE1 activity was sufficient to restore CDC2 activity and promote G_2/M entry and transition and cellular proliferation, indicating that the NHE1-driven increase in pH_i is an important checkpoint for progression to G_2 phase of the cell cycle and mitosis.[68] We speculate that IL-13 induction of *SLC9A3*/NHE3 might be a critical requirement for esophageal epithelial cell proliferation through regulating pH_i.

Notably, we have demonstrated previously that overexpression of IL-13 in mice leads to esophageal cell proliferation.[69] Here we show colocalization of NHE3 expression within the esophageal basal proliferative zone in esophageal biopsy samples from patients with EoE and IL-13–treated EPC2-ALI cultures. Furthermore, we show that stimulating EPC2-ALI cells with IL-13 induces *SLC9A3*, but not *SLC9A1* expression and that treating mature EPC2-ALI cells with the pan-NHE inhibitor ethylisopropylamiloride attenuated IL-13–induced proliferation (see Fig E3 in this article's Online Repository at www.jacionline.org). These findings support the necessity of an NHE in IL-13–induced proliferation in an esophageal epithelial model system *in vitro*, and given the overexpression, localization, and function of NHE3, we conjecture that pH_i balance is a critical

component of the proliferative response induced by IL-13 and is mediated by an NHE in esophageal epithelial cells.

Multiple compensatory mechanisms regulate pH_i in mammalian cells and involve Na^+/H^+ exchangers, HCO_3^- transporters, lactate-H^+ transporters, and vacuolar H^+-ATPase.[70,71] Our GO analysis supports dysregulation of these mechanisms in patients with EoE, identifying that 5 of the 50 individual GO nodes generated from genes significantly dysregulated in patients with EoE are correlated tightly with the transmembrane ion transport activity. Notably, several of the most dysregulated genes were part of the pH_i regulatory circuit, including Cl^-/HCO_3^- exchangers (*SLC26A4*, *SLC4A2*, and *SLC4A8*) and carbonic anhydrases. These functional analyses support the concept of pH_i pathways being active in primary esophageal epithelial cells in patients with EoE.

The demonstration that a significant decrease in DIS with steroid therapy or elimination diet in patients with EoE is associated with symptom improvement[31] indicates an association between DIS and the cause of EoE. We demonstrate a role for *SLC9A3*/NHE3 and Na^+/H^+ exchange in DIS formation, one of the histopathologic manifestations of EoE. Given our observations, one would predict that using NHE3 antagonists (systemically or topically) might be a therapeutic approach for reducing DIS and thus normalizing associated esophageal caliber in patients with EoE. Notably, the NHE3-specific inhibitor tenapanor is in phase 3 clinical trials for the treatment of cardiorenal and gastrointestinal disease.[72] Tenapanor has been shown to reduce sodium uptake, resulting in reduction in pH_i.[72] Given the contribution of DIS to esophageal barrier dysfunction and facilitating food allergen exposure, considering potential use of NHE3 inhibitors for EoE is warranted.

In summary, we identified a relationship between *SLC9A3*/NHE3 expression and activity with DIS in patients with EoE. Mechanistically, we show that IL-13 stimulates *SLC9A3* expression and NHE3 activity (through pH_i) and that these were associated with esophageal epithelial DIS. Inhibiting NHE activity attenuated esophageal epithelial DIS formation, providing rationale for the therapeutic use of NHE3 antagonists for reducing DIS and DIS-associated esophageal pathophysiologic manifestations in patients with EoE.

Key messages

- **The EoE transcriptome consists of altered expression of gene networks associated with regulation of pH_i and acid-protective mechanisms.**
- **There is increased expression of *SLC9A3* within the basal layer of esophageal biopsy specimens from patients with EoE, and this expression correlated positively with disease severity (eosinophils/hpf) and DIS.**
- **IL-13–induced *SLC9A3* expression and Na^+-dependent proton secretion and SLC9A3 activity correlated positively with DIS formation.**
- **IL-13–mediated Na^+-dependent proton secretion was the primary intracellular acid-protective mechanism within the esophageal epithelium.**
- **SLC9A3-dependent transport is required for IL-13–induced DIS formation.**

REFERENCES

1. Dellon ES, Hirano I. Epidemiology and natural history of eosinophilic esophagitis. Gastroenterology 2018;154:319-22.e3.
2. Dellon ES. Epidemiology of eosinophilic esophagitis. Gastroenterol Clin North Am 2014;43:201-18.
3. Prasad GA, Alexander JA, Schleck CD, Zinsmeister AR, Smyrk TC, Elias RM, et al. Epidemiology of eosinophilic esophagitis over three decades in Olmsted County, Minnesota. Clin Gastroenterol Hepatol 2009;7:1055-61.
4. Arias A, Perez-Martinez I, Tenias JM, Lucendo AJ. Systematic review with meta-analysis: the incidence and prevalence of eosinophilic oesophagitis in children and adults in population-based studies. Aliment Pharmacol Ther 2016; 43:3-15.
5. Liacouras CA, Furuta GT, Hirano I, Atkins D, Attwood SE, Bonis PA, et al. Eosinophilic esophagitis: updated consensus recommendations for children and adults. J Allergy Clin Immunol 2011;128:3-22.e6.
6. Klinnert MD, Silveira L, Harris R, Moore W, Atkins D, Fleischer DM, et al. Health-related quality of life over time in children with eosinophilic esophagitis and their families. J Pediatr Gastroenterol Nutr 2014;59:308-16.
7. Akei HS, Mishra A, Blanchard C, Rothenberg ME. Epicutaneous antigen exposure primes for experimental eosinophilic esophagitis in mice. Gastroenterology 2005;129:985-94.
8. Collins MH. Histopathology of eosinophilic esophagitis. Dig Dis 2014;32:68-73.
9. Collins MH. Histopathologic features of eosinophilic esophagitis. Gastrointest Endosc Clin North Am 2008;18:59-71, viii-ix.
10. Doherty TA, Baum R, Newbury RO, Yang T, Dohil R, Aquino M, et al. Group 2 innate lymphocytes (ILC2) are enriched in active eosinophilic esophagitis. J Allergy Clin Immunol 2015;136:792-4.e3.
11. Abu-Sultaneh SM, Durst P, Maynard V, Elitsur Y. Fluticasone and food allergen elimination reverse sub-epithelial fibrosis in children with eosinophilic esophagitis. Dig Dis Sci 2011;56:97-102.
12. Straumann A, Conus S, Degen L, Felder S, Kummer M, Engel H, et al. Budesonide is effective in adolescent and adult patients with active eosinophilic esophagitis. Gastroenterology 2010;139:1526-37.e1.
13. Arora AS, Perrault J, Smyrk TC. Topical corticosteroid treatment of dysphagia due to eosinophilic esophagitis in adults. Mayo Clin Proc 2003;78: 830-5.
14. Faubion WA Jr, Perrault J, Burgart LJ, Zein NN, Clawson M, Freese DK. Treatment of eosinophilic esophagitis with inhaled corticosteroids. J Pediatr Gastroenterol Nutr 1998;27:90-3.
15. Kelly KJ, Lazenby AJ, Rowe PC, Yardley JH, Perman JA, Sampson HA. Eosinophilic esophagitis attributed to gastroesophageal reflux: improvement with an amino acid-based formula. Gastroenterology 1995;109:1503-12.
16. Liacouras CA, Ruchelli E. Eosinophilic esophagitis. Curr Opin Pediatr 2004;16: 560-6.
17. Liacouras CA, Wenner WJ, Brown K, Ruchelli E. Primary eosinophilic esophagitis in children: successful treatment with oral corticosteroids. J Pediatr Gastroenterol Nutr 1998;26:380-5.
18. Blanchard C, Mingler MK, Vicario M, Abonia JP, Wu YY, Lu TX, et al. IL-13 involvement in eosinophilic esophagitis: transcriptome analysis and reversibility with glucocorticoids. J Allergy Clin Immunol 2007;120:1292-300.
19. Mishra A, Hogan SP, Brandt EB, Rothenberg ME. IL-5 promotes eosinophil trafficking to the esophagus. J Immunol 2002;168:2464-9.
20. Mishra A, Hogan SP, Brandt EB, Rothenberg ME. An etiological role for aeroallergens and eosinophils in experimental esophagitis. J Clin Invest 2001; 107:83-90.
21. Mishra A, Rothenberg ME. Intratracheal IL-13 induces eosinophilic esophagitis by an IL-5, eotaxin-1, and STAT6-dependent mechanism. Gastroenterology 2003;125:1419-27.
22. Blanchard C, Stucke EM, Burwinkel K, Caldwell JM, Collins MH, Ahrens A, et al. Coordinate interaction between IL-13 and epithelial differentiation cluster genes in eosinophilic esophagitis. J Immunol 2010;184:4033-41.
23. Blanchard C, Stucke EM, Rodriguez-Jimenez B, Burwinkel K, Collins MH, Ahrens A, et al. A striking local esophageal cytokine expression profile in eosinophilic esophagitis. J Allergy Clin Immunol 2011;127:208-17, e1-7.
24. Sherrill JD, Kiran KC, Blanchard C, Stucke EM, Kemme KA, Collins MH, et al. Analysis and expansion of the eosinophilic esophagitis transcriptome by RNA sequencing. Genes Immun 2014;15:361-9.
25. Rothenberg ME, Wen T, Greenberg A, Alpan O, Enav B, Hirano I, et al. Intravenous anti-IL-13 mAb QAX576 for the treatment of eosinophilic esophagitis. J Allergy Clin Immunol 2015;135:500-7.
26. D'Mello RJ, Caldwell JM, Azouz NP, Wen T, Sherrill JD, Hogan SP, et al. LRRC31 is induced by IL-13 and regulates kallikrein expression and barrier function in the esophageal epithelium. Mucosal Immunol 2016;9:744-56.

27. Davis BP, Stucke EM, Khorki ME, Litosh VA, Rymer JK, Rochman M, et al. Eosinophilic esophagitis-linked calpain 14 is an IL-13-induced protease that mediates esophageal epithelial barrier impairment. JCI Insight 2016;1:e86355.
28. Sherrill JD, Kc K, Wu D, Djukic Z, Caldwell JM, Stucke EM, et al. Desmoglein-1 regulates esophageal epithelial barrier function and immune responses in eosinophilic esophagitis. Mucosal Immunol 2014;7:718-29.
29. Purdy JK, Appelman HD, Golembeski CP, McKenna BJ. Lymphocytic esophagitis: a chronic or recurring pattern of esophagitis resembling allergic contact dermatitis. Am J Clin Pathol 2008;130:508-13.
30. Caviglia R, Ribolsi M, Maggiano N, Gabbrielli AM, Emerenziani S, Guarino MP, et al. Dilated intercellular spaces of esophageal epithelium in nonerosive reflux disease patients with physiological esophageal acid exposure. Am J Gastroenterol 2005;100:543-8.
31. Ravelli A, Villanacci V, Cadei M, Fuoti M, Gennati G, Salemme M. Dilated intercellular spaces in eosinophilic esophagitis. J Pediatr Gastroenterol Nutr 2014;59:589-93.
32. Mueller S, Neureiter D, Aigner T, Stolte M. Comparison of histological parameters for the diagnosis of eosinophilic oesophagitis versus gastro-oesophageal reflux disease on oesophageal biopsy material. Histopathology 2008;53:676-84.
33. Orlowski J, Grinstein S. Emerging roles of alkali cation/proton exchangers in organellar homeostasis. Curr Opin Cell Biol 2007;19:483-92.
34. Trapnell C, Roberts A, Goff L, Pertea G, Kim D, Kelley DR, et al. Differential gene and transcript expression analysis of RNA-seq experiments with TopHat and Cufflinks. Nat Protoc 2012;7:562-78.
35. Langmead B, Trapnell C, Pop M, Salzberg SL. Ultrafast and memory-efficient alignment of short DNA sequences to the human genome. Genome Biol 2009; 10:R25.
36. Garber M, Grabherr MG, Guttman M, Trapnell C. Computational methods for transcriptome annotation and quantification using RNA-seq. Nat Methods 2011; 8:469-77.
37. Kartashov AV, Barski A. BioWardrobe: an integrated platform for analysis of epigenomics and transcriptomics data. Genome Biol 2015;16:158.
38. Chen J, Bardes EE, Aronow BJ, Jegga AG. ToppGene Suite for gene list enrichment analysis and candidate gene prioritization. Nucleic Acids Res 2009; 37:W305-11.
39. Harada H, Nakagawa H, Oyama K, Takaoka M, Andl CD, Jacobmeier B, et al. Telomerase induces immortalization of human esophageal keratinocytes without p16(INK4a) inactivation. Mol Cancer Res 2003;1:729-38.
40. Schwark JR, Jansen HW, Lang HJ, Krick W, Burckhardt G, Hropot M. S3226, a novel inhibitor of Na+/H+ exchanger subtype 3 in various cell types. Pflugers Arch 1998;436:797-800.
41. Iovannisci D, Illek B, Fischer H. Function of the HVCN1 proton channel in airway epithelia and a naturally occurring mutation, M91T. J Gen Physiol 2010;136:35-46.
42. Wakabayashi S, Shigekawa M, Pouyssegur J. Molecular physiology of vertebrate Na+/H+ exchangers. Physiol Rev 1997;77:51-74.
43. Liu Y, Munker S, Mullenbach R, Weng HL. IL-13 signaling in liver fibrogenesis. Front Immunol 2012;3:116.
44. Amin MR, Malakooti J, Sandoval R, Dudeja PK, Ramaswamy K. IFN-gamma and TNF-alpha regulate human NHE3 gene expression by modulating the Sp family transcription factors in human intestinal epithelial cell line C2BBe1. Am J Physiol Cell Physiol 2006;291:C887-96.
45. Clayburgh DR, Musch MW, Leitges M, Fu YX, Turner JR. Coordinated epithelial NHE3 inhibition and barrier dysfunction are required for TNF-mediated diarrhea in vivo. J Clin Invest 2006;116:2682-94.
46. Su HW, Wang SW, Ghishan FK, Kiela PR, Tang MJ. Cell confluency-induced Stat3 activation regulates NHE3 expression by recruiting Sp1 and Sp3 to the proximal NHE3 promoter region during epithelial dome formation. Am J Physiol Cell Physiol 2009;296:C13-24.
47. Rochman M, Kartashov AV, Caldwell JM, Collins MH, Stucke EM, Kc K, et al. Neurotrophic tyrosine kinase receptor 1 is a direct transcriptional and epigenetic target of IL-13 involved in allergic inflammation. Mucosal Immunol 2015;8:785-98.
48. Cho SJ, Kang MJ, Homer RJ, Kang HR, Zhang X, Lee PJ, et al. Role of early growth response-1 (Egr-1) in interleukin-13-induced inflammation and remodeling. J Biol Chem 2006;281:8161-8.
49. Malakooti J, Sandoval R, Amin MR, Clark J, Dudeja PK, Ramaswamy K. Transcriptional stimulation of the human NHE3 promoter activity by PMA: PKC independence and involvement of the transcription factor EGR-1. Biochem J 2006;396:327-36.
50. Brant SR, Yun CH, Donowitz M, Tse CM. Cloning, tissue distribution, and functional analysis of the human Na+/N+ exchanger isoform, NHE3. Am J Physiol Cell Physiol 1995;269:C198-206.
51. Praetorius J, Andreasen D, Jensen BL, Ainsworth MA, Friis UG, Johansen T. NHE1, NHE2, and NHE3 contribute to regulation of intracellular pH in murine duodenal epithelial cells. Am J Physiol Gastrointest Liver Physiol 2000;278: G197-206.
52. Wang Z, Orlowski J, Shull GE. Primary structure and functional expression of a novel gastrointestinal isoform of the rat Na/H exchanger. J Biol Chem 1993;268: 11925-8.
53. Schultheis PJ, Clarke LL, Meneton P, Miller ML, Soleimani M, Gawenis LR, et al. Renal and intestinal absorptive defects in mice lacking the NHE3 Na+/H+ exchanger. Nat Genet 1998;19:282-5.
54. Swietach P, Vaughan-Jones RD, Harris AL, Hulikova A. The chemistry, physiology and pathology of pH in cancer. Philos Trans R Soc Lond B Biol Sci 2014;369:20130099.
55. Orlando RC. Esophageal mucosal defense mechanisms. GI Motility Online 2006; https://doi.org/10.1038/gimo15.
56. Tobey NA, Gambling TM, Vanegas XC, Carson JL, Orlando RC. Physicochemical basis for dilated intercellular spaces in non-erosive acid-damaged rabbit esophageal epithelium. Dis Esophagus 2008;21:757-64.
57. Orlando LA, Orlando RC. Dilated intercellular spaces as a marker of GERD. Curr Gastroenterol Rep 2009;11:190-4.
58. Noffsinger AE. Update on esophagitis: controversial and underdiagnosed causes. Arch Pathol Lab Med 2009;133:1087-95.
59. Barlow WJ, Orlando RC. The pathogenesis of heartburn in nonerosive reflux disease: a unifying hypothesis. Gastroenterology 2005;128:771-8.
60. Collins MH, Martin LJ, Alexander ES, Boyd JT, Sheridan R, He H, et al. Newly developed and validated eosinophilic esophagitis histology scoring system and evidence that it outperforms peak eosinophil count for disease diagnosis and monitoring. Dis Esophagus 2017;30:1-8.
61. Rodrigo J, Hernandez DJ, Vidal MA, Pedrosa JA. Vegetative innervation of the esophagus III. Intraepithelial endings. Acta Anat 1975;92:242.
62. Pouyssegur J, Franchi A, L'Allemain G, Paris S. Cytoplasmic pH, a key determinant of growth factor-induced DNA synthesis in quiescent fibroblasts. FEBS Lett 1985;190:115-9.
63. Schelling JR, Abu Jawdeh BG. Regulation of cell survival by Na+/H+ exchanger-1. Am J Physiol Renal Physiol 2008;295:F625-32.
64. Moolenaar WH, Defize LH, De Laat SW. Ionic signalling by growth factor receptors. J Exp Biol 1986;124:359-73.
65. Di Sario A, Svegliati Baroni G, Bendia E, Ridolfi F, Saccomanno S, Ugili L, et al. Intracellular pH regulation and Na+/H+ exchange activity in human hepatic stellate cells: effect of platelet-derived growth factor, insulin-like growth factor 1 and insulin. J Hepatol 2001;34:378-85.
66. Li M, Morley P, Asem EK, Tsang BK. Epidermal growth factor elevates intracellular pH in chicken granulosa cells. Endocrinology 1991;129: 656-62.
67. Vairo G, Cocks BG, Cragoe EJ Jr, Hamilton JA. Selective suppression of growth factor-induced cell cycle gene expression by Na+/H+ antiport inhibitors. J Biol Chem 1992;267:19043-6.
68. Putney LK, Barber DL. Na-H exchange-dependent increase in intracellular pH times G2/M entry and transition. J Biol Chem 2003;278:44645-9.
69. Zuo L, Fulkerson PC, Finkelman FD, Mingler M, Fischetti CA, Blanchard C, et al. IL-13 induces esophageal remodeling and gene expression by an eosinophil-independent, IL-13R alpha 2-inhibited pathway. J Immunol 2010; 185:660-9.
70. Schreiber R. Ca2+ signaling, intracellular pH and cell volume in cell proliferation. J Membr Biol 2005;205:129-37.
71. Shrode LD, Tapper H, Grinstein S. Role of intracellular pH in proliferation, transformation, and apoptosis. J Bioenerg Biomembr 1997;29:393-9.
72. Spencer AG, Labonte ED, Rosenbaum DP, Plato CF, Carreras CW, Leadbetter MR, et al. Intestinal inhibition of the Na+/H+ exchanger 3 prevents cardiorenal damage in rats and inhibits Na+ uptake in humans. Sci Transl Med 2014;6:227ra36.